

# Understanding Weathering of Oil Sands Ores by Atomic Force Microscopy

Sili Ren, Hongying Zhao, Jun Long, Zhenghe Xu, and Jacob Masliyah

Department of Chemical and Materials Engineering, University of Alberta, Edmonton, AB, Canada

DOI 10.1002/aic.12000

Published online August 24, 2009 in Wiley InterScience (www.interscience.wiley.com).

*Effect of weathering on colloidal interactions between bitumen and oil sands solids was studied by atomic force microscopy (AFM). The change in bitumen chemistry due to weathering was found to have a negligible effect on the interactions of bitumen with solid particles. However, the increase in solid surface hydrophobicity due to ore weathering reversed the long-range interaction forces between bitumen and solids from repulsive to attractive with a corresponding increase in adhesion force. The measured force profiles between bitumen and various solids can be well fitted with the extended DLVO theory by considering an additional attractive force. The attractive long-range force and increased adhesion force make the separation of bitumen from solids more difficult and the attachment of fine solids on liberated bitumen easier, thereby leading to poor bitumen liberation and lower aeration efficiency. Such changes account for the observed poor processability of the weathered ores. © 2009 American Institute of Chemical Engineers AICHE J, 55: 3277–3285, 2009*

**Keywords:** oil sands, bitumen extraction, colloidal forces, atomic force microscopy, weathered ores

## Introduction

Alberta in Canada owns the second largest oil reserve world-wide, locked in oil sands deposits. Among the vast oil sands deposits, the weathered/oxidized oil sands ore is characterized by low bitumen recovery and poor bitumen froth quality when processed using a water-based extraction process.<sup>1–6</sup> Understanding the processability of weathered/oxidized ores has attracted much attention during last several decades. Early studies attributed the poor processability of weathered/oxidized ores to oxidation of minerals in the ores, resulting in solubilization of inorganic salts and causing a high polyvalent cation concentration in the aqueous phase.<sup>1,3,4</sup> However, a recent study reported that the poor processability of the weathered/oxidized ore was a result of changes in bitumen chemistry during ore weathering/aging.<sup>2</sup> Clearly, the mechanisms of oil sands weathering in the context of their poor processability remain controversial and to be established.

Oil sand processing using water-based extraction processes is known to involve two essential steps: 1) bitumen liberation from the sand grains and 2) bitumen aeration followed by flotation to form a bitumen-rich froth.<sup>7,8</sup> Bitumen liberation is controlled by bitumen–solids interactions, whereas bitumen aeration is determined mainly by the hydrophobicity of the bitumen surface and heterocoagulation of bitumen with fine solids.<sup>8,9</sup> Therefore, investigation on colloidal interactions between bitumen and oil sands solids is important to understand the bitumen extraction process. Atomic force microscopy (AFM) colloid probe technique has been successfully used to measure the interaction forces between the various components in oil sands. Such studies have provided insights into the mechanisms of bitumen extraction.<sup>8–15</sup> Extensive studies have shown that oil sands processability is closely related to the colloidal interactions between bitumen and solids.<sup>6,9,10,16</sup> A strong long-range repulsive force and weak adhesion between bitumen and solids generally correspond to a good processability, whereas a long-range attractive force and strong adhesion correspond to a poor processability.<sup>6,16</sup> With the early success of applying colloid probe technique to understanding of oil sand processability, the same technique was used to explore the nature of ore

Correspondence concerning this article should be addressed to H. Zhao hzhao@ualberta.ca

**Table 1. Composition of the Oil Sand Ores Used**

Type of Ore		Composition (wt%)				Supplier
		Bitumen	Water	Solids	Fines in Solids <44 $\mu\text{m}$	
Good Processing Ore	GPO	14.3	3.4	82.3	12.7	Synchrude, Fort McMurray, Canada
Laboratory Weathered Ore	LWO	14.2	0.2	85.6	12.7	Weathered in-house
Naturally Weathered Ore	NWO	12.2	2.6	85.2	12.4	Suncor, Fort McMurray, Canada

weathering effect on oil sands processability by measuring the interaction forces between bitumen and fine solids isolated from the weathered ores.

In a previous study,<sup>17</sup> it was shown that oil sands weathering caused organic materials to adsorb onto the mineral solid surfaces, greatly increasing their surface hydrophobicity. It was anticipated that such adsorption and changes in the solid surface properties would affect the interactions between the solids and bitumen, and consequently the processability of oil sands ores. In this article, atomic force microscopy (AFM) was employed to directly measure the interaction forces between bitumen and various solids and to study the effect of weathering on the interactions. Based on the measured forces, how weathering affects ore processability was discussed and possible coping strategies to improve the processability of weathered ores were explored.

## Experimental

### Materials

Three ores, including a good processing ore (GPO), a laboratory weathered ore (LWO), and a naturally weathered ore (NWO) as used in our previous communication,<sup>17</sup> were used in this work. LWO was obtained by weathering the GPO in an oven at 60°C with air ventilation for 7 days. The details on laboratory oil sands weathering were described in our previous communication.<sup>17</sup> The composition of the various ores is given in Table 1.

As a model for good processing oil sands grains, hydrophilic silica spheres of  $\sim 8\ \mu\text{m}$  in diameter were well mixed with a small amount of the GPO and were subsequently extracted using toluene washing. They are defined as non-weathered model silica and referred to as “Silica 2” in Table 2. As a model for weathered oil sands grains, the model silica spheres mixed with the GPO were weathered in the oven under the same conditions as laboratory weathering of ores. They are defined as weathered model silica and referred to as “Silica 3” (Table 2). Fine solids were also isolated from different ores by toluene washing. These solids are described in Table 2 and referred to as mineral solids of about  $10\ \mu\text{m}$  in diameter. The toluene washing procedure has been described in our previous communication.<sup>17</sup> Briefly, after the addition of toluene to the ore and shaking the mixture for several minutes, the mixture was centrifuged at 20,000g force for 30 min. The upper bitumen solution was collected and adjusted to desired concentrations by adding toluene for preparing bitumen film on silicon wafers. Repetitive washing of the solids with toluene was conducted until the supernatant became colorless. The solid particles were then collected and dried in a vacuum oven at room temperature.

Plant recycle process water (PW) supplied by Syncrude Canada was used as the liquid medium in the force measure-

ments. The major ionic components of the process water are given in Table 3.

### Force measurements

The colloidal forces were measured using an atomic force microscope (AFM, Digital Instrument, Santa Barbara, CA). AFM probes were prepared by gluing a fine solid particle onto a standard silicone nitride AFM cantilever (Digital Instruments, CA). The cantilever with a nominal spring constant of 0.58 N/m was chosen. The spring constant of the cantilever was calibrated by thermal tune method. The prepared probe was kept in a particle-free environment for over 12 h prior to its use in force measurements. SEM micrographs of a model silica probe and a fine particle isolated from the good processing ore are shown in Figure 1. The model silica probe is spherical in shape and smooth, whereas the fine particle from the good processing ore is irregular in shape and quite rough. The radius of the particle was determined from an SEM image after the force measurements. A circle was drawn to enclose a near-spherical particle. The radius of the circle was determined and used as the radius of the particle.

Single-crystal silicon wafers (Silicon Valley Microelectronics, Santa Clara, CA) were cut into  $12 \times 12\ \text{mm}^2$  pieces which were used as substrate for preparing bitumen surfaces. Before bitumen coating, the substrates were cleaned by immersing them in a piranha solution (a mixture of 7:3 (V/V) 98%  $\text{H}_2\text{SO}_4$  and 30%  $\text{H}_2\text{O}_2$ ) at 90°C for 30 min, then rinsed with ultra-pure water and dried by nitrogen blow. The silicon substrates cleaned as such were hydrophilic with a

**Table 2. Types of Solid Particles Used in the AFM Force Measurements**

Type of Solid Particles		Preparation Method
Silica 1	Original model silica	Commercial silica spheres or substrate as received
Silica 2	Nonweathered model silica	Silica 1 mixed with good processing ore (GPO) or contacted with bitumen and washed by toluene
Silica 3	Weathered model silica	Silica 1 mixed with GPO or contacted with bitumen, weathered in oven and then washed by toluene
Fines 1	Good ore fines	Toluene-solvent-extracted from GPO
Fines 2	Laboratory weathered ore fines	Toluene-solvent-extracted from laboratory weathered ore (LWO)
Fines 3	Naturally weathered ore fines	Toluene-solvent-extracted from naturally weathered ore (NWO)

**Table 3. Concentration (mg/L) of Various Ions in the Plant Process Water**

Ions	Na <sup>+</sup>	K <sup>+</sup>	Ca <sup>2+</sup>	Mg <sup>2+</sup>	Fe <sup>2+/3+</sup>	Cl <sup>-</sup>	SO <sub>4</sub> <sup>2-</sup>	HCO <sub>3</sub> <sup>-</sup>
Concentration	544	20	27	17	0.04	368	95	620

water contact angle of almost 0°. To ensure bitumen layer sticking on the substrate, the hydrophilic substrates were modified with a self-assembled monolayer of alkylsilanes using a well-established method described elsewhere.<sup>18,19</sup> Briefly, the silicon substrates were placed in a  $5.0 \times 10^{-3}$  M TMCS-in-toluene (TMCS: 98% trimethylchlorosilane, purchased from Aldrich, Canada) solution for 6 h. After being rinsed with toluene, the silanized silicon substrates became relative hydrophobic with a water contact angle of about 78°. The hydrophobized substrates were used to prepare bitumen surface by spin-coating method, which was described in our previous communication.<sup>17</sup> A WS-400A-6NPP/LITE spin coater (Laurell Technologies Co., North Wales, PA) was used.

The interaction forces between a solid particle and a bitumen surface in an aqueous medium were measured.<sup>16</sup> Prior to data collection, both the probe and bitumen surface were immersed in the test liquid sealed in a fluid cell for at least 30 min to equilibrate the system. In AFM force measurements, the long-range interaction forces are recorded when the probe approaches the substrate surface, whereas the pull-off force is measured as the probe retracts from the substrate. The pull-off force needed to detach the probe from the substrate surface is regarded as the adhesion force. To obtain representative results, at least six different bitumen-particle pairs are used for each test condition. For a clear presentation, only one typical long-range force profile for each test condition is presented in this article. The adhesion force for each test condition is the statistical value determined using at least 100 retraction force profiles. For a quantitative comparison, the measured long-range interaction force ( $F$ ) and adhesion force ( $F_{adh}$ ) are normalized by the probe particle radius ( $R$ ). All experiments are conducted at room temperature,  $22 \pm 1^\circ\text{C}$ .

### Zeta potential measurements

Zeta potentials of the silica particles and bitumen samples were measured using a Zetaphoremeter III apparatus (SEPHY-CAD Instrumentations, France). Silica powders

from Duke Scientific were used in zeta potential distribution measurement. Silica suspension was prepared by adding 0.1 g of silica powder in 100 ml of 1 mM KCl solution or plant process water. The mixture was ultrasonicated in a water bath for 5 min, followed by 1 h equilibration. The pH of the prepared suspension was adjusted to 8.0–8.6 prior to zeta-potential measurement. A detailed description of the instrument and measurement procedures can be found elsewhere.<sup>15,20</sup>

## Results

The interaction forces between bitumen and solids play a significant role in oil sands processing. Essentially, they control the “liberation” of bitumen from the sand grains and bitumen aeration which in turn determine bitumen recovery and bitumen froth quality.<sup>8,9</sup> To better understand the processability of the weathered ore, the long-range interactions and adhesion forces between a bitumen surface and a fine solid particle were measured using the AFM colloidal probe technique. To determine the impact of bitumen chemistry on processability of weathered ores, measurements were performed using bitumen extracted from the GPO, LWO and NWO for a given silica probe. For comparison, bitumen obtained from commercial oil sands operation was also used. The model silica probe in the force measurements was cleaned by UV radiation prior to its use. The results in Figure 2, obtained at pH 8.0–8.6, show almost identical long-range force profiles, independent of the source of bitumen. The measured repulsion in 1 mM KCl aqueous solutions (Figure 2a) was much stronger than in plant process water (Figure 2b). In both cases, the adhesion force between bitumen and silica probe was found negligible. These observations suggest that different sources of bitumen have a negligible effect on bitumen–silica interactions although the bitumen chemistry was found slightly changed during weathering as discussed in our previous communication.<sup>17</sup> Because the different source of bitumen showed a negligible effect on the interaction forces, commercially extracted bitumen was used for the remainder of force measurements and our focus turned to the solids.

The interaction of commercially extracted bitumen with different silica particles, as described in Table 2, was measured. The results in Figure 3 show drastically different force profiles for the original, nonweathered, and weathered silica spheres. In 1mM KCl solutions (Figure 3a), for example, a

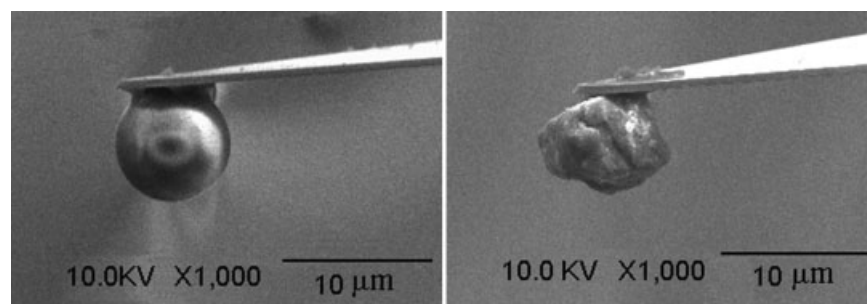


**Figure 1. SEM micrographs of a model silica (left) and a fine particle (right) from an oil sand ore glued on AFM cantilevers.**

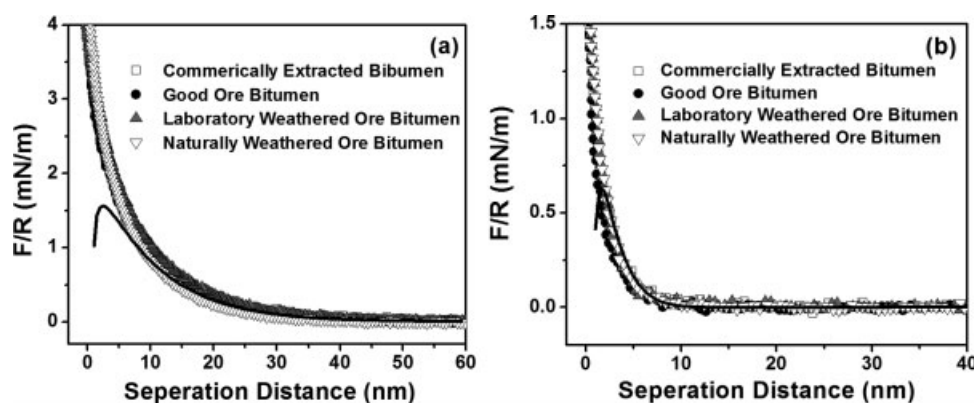


**Figure 2.** Normalized long-range interaction forces ( $F/R$ ) between a model silica and various bitumen surfaces as a function of separation distance in (a) 1 mM KCl solutions and (b) plant process water at pH = 8.0–8.6. Solid lines represent the calculated DLVO interaction force profiles.

strong monotonic repulsive force profile with near-zero adhesion was observed for the original model silica (Silica 1) interacting with bitumen. In contrast, for the nonweathered silica (Silica 2), the repulsive forces decreased to some extent and a jump-in at a separation distance of around 7 nm was observed. With a relatively high repulsive force barrier, only a weak adhesion force of about 3.5 mN/m was measured. For the weathered silica probe (Silica 3), the repulsive force barrier became very small with a much longer jump-in distance of about 12 nm. The adhesion force in this case further increased to 8.5 mN/m. The results indicate a strong impact on the model silica sphere surface properties due to its mixing with the GPO without weathering and more so with weathering. The presence of attractive forces and strong adhesion forces due to ore weathering makes bitumen liberation from the sand grains difficult, leading to a negative effect on bitumen recovery of the weathered ore. Similar trend was observed for bitumen–silica interactions in plant process water as shown in Figure 3b, although the measured long-range repulsive forces were greatly depressed and the corresponding adhesion forces reduced. The observed

decrease of both long-range repulsion and adhesion forces in the plant process water than in 1 mM KCl is attributed to higher ionic strength of the plant process water.<sup>15</sup>

The force measurement was extended to real fine solids extracted from various ores. Because of the irregular surface characteristic and the roughness of the fine solids (Figure 1), the measured interaction force profiles between bitumen and various fine solids were found scattered within a certain range. As an example, Figure 4 shows the interaction force profiles for the fine solids isolated from the same good processing ore, GPO, interacting with a bitumen substrate in 1 mM KCl aqueous solutions. For clear presentation, only one representative curve will be shown in the subsequent discussions for each measurement condition. The long-range interaction and adhesion forces measured between bitumen and fine solids isolated from various ores are shown in Figure 5. In 1 mM KCl solution (Figure 5a), a relatively high repulsive force barrier with a jump-in at around 7 nm and weak adhesion (ca. 2.9 mN/m) were obtained for the fine solids from the good processing ore. In contrast, for fines from the laboratory and naturally weathered ores, the repulsive force

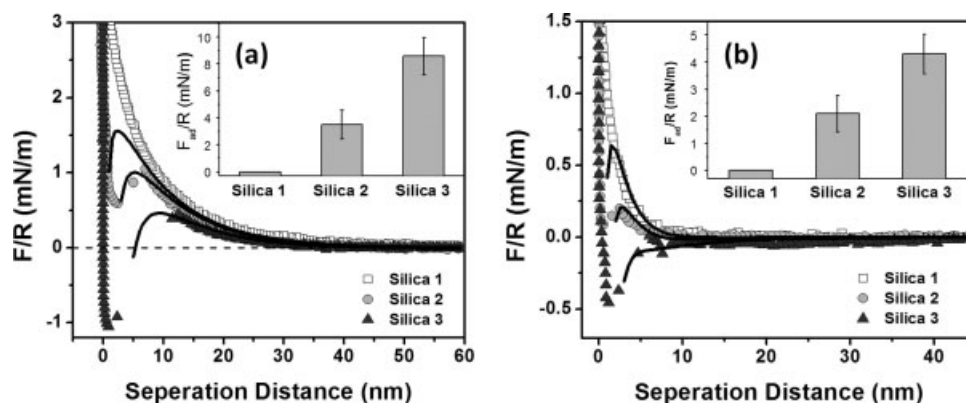


**Figure 3.** Normalized long-range interaction forces ( $F/R$ ) of bitumen interacting with model silica (Silica 1), non-weathered model silica (Silica 2), and weathered model silica (Silica 3) as a function of separation distance in (a) 1 mM KCl solution and (b) plant process water at pH = 8.0–8.6. Solid lines represent the best fitted interaction force profiles with the extended DLVO theory. Inset shows the corresponding normalized adhesion forces.



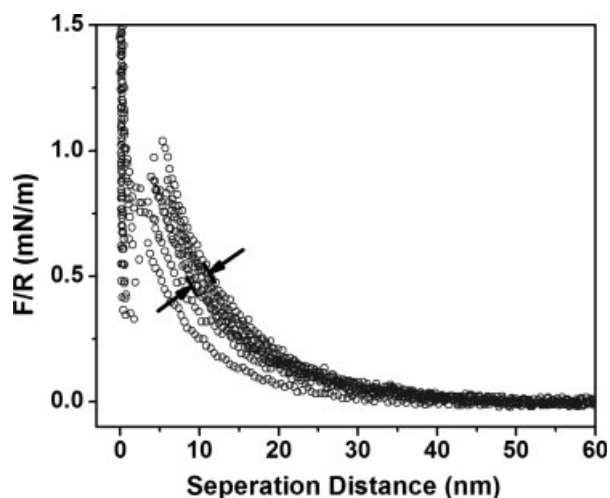


**Figure 4. Normalized long-range force profiles measured between bitumen and fine solids isolated from good processing ore.**

The measurements were conducted in 1 mM KCl solutions at pH = 8.0–8.6. A representative force curve was selected within the region where the arrows pointed for comparison with other bitumen-fine solids interaction force profiles.

barriers became very low with a jump-in at a much larger separation distance of 10–15 nm. They are accompanied by a strong adhesion force of 9.3 and 8.2 mN/m, respectively. Compared with those force profiles obtained in the 1 mM KCl solution, the long-range forces in the plant process water (Figure 5b) were depressed significantly due to higher ionic strength of the process water. The average adhesion forces were also decreased in the plant process water, from 2.9 to 1.2, 9.3 to 4.0, and 8.2 to 3.7 mN/m for fine solids extracted from GPO, LWO, and NWO, respectively. The results from the colloidal force measurements suggest a change of fine solids surface properties by laboratory weathering of the good processing ore that led to a reversal in the long-range forces. Here, the repulsive long-range forces between bitumen and fines became attractive with higher ad-

hesion forces, a characteristic similar to naturally weathered ores.

Our previous study showed that weathering led to adsorption of organic materials onto solid surfaces, making the solid particles more hydrophobic.<sup>17</sup> Such a change in surface hydrophobicity is believed to be responsible for the significant change of the colloidal forces between the bitumen and fine solids. If this is the case, removal of the organic materials from the solid surface is anticipated to restore the colloidal forces to their original profiles. To verify this hypothesis, the weathered model silica probe (Silica 3) were exposed to a UV light for over 12 h and then used to measure the colloidal forces. The UV radiation was intended to remove the organic materials on the silica surface and restore the hydrophilic nature of the silica spheres. As shown in Figure 6a, the UV radiation of the weathered model silica probe restored interaction force profiles to the force profiles of original silica probe, i.e., long-range forces returned to monotonically repulsive and adhesion force disappeared. Similar restoration by UV-radiation was observed for oil sands fine solids (Figure 6b). It is evident that increasing surface hydrophilicity by removing organic contaminants from the solid surfaces can control the colloidal forces between bitumen and sand grains or fine solids, thereby improving the processability of the weathered ore.

Although it is not practical to remove organic contaminants from solids by UV radiation in oil sands processing, our previous study showed that one can partially remove organic matter from solid surface by hot water washing.<sup>17</sup> To show whether such an approach would be effective in changing solids hydrophobicity to affect colloidal forces, the fine solids extracted from laboratory weathered ore were washed in hot water of 40, 65, and 100°C for 15 min prior to gluing the fine particle on an AFM cantilever. The results in Figure 7 show a progressive decrease in long-range attractive force and gradual increase in repulsive force barrier with increasing washing temperature above 65°C. The adhesion force, on the other hand, decreased progressively to 5.8, 3.7, and 0.7 mN/m for the solids washed at 40, 65, and 100°C, respectively. Such changes in long-range force profiles and

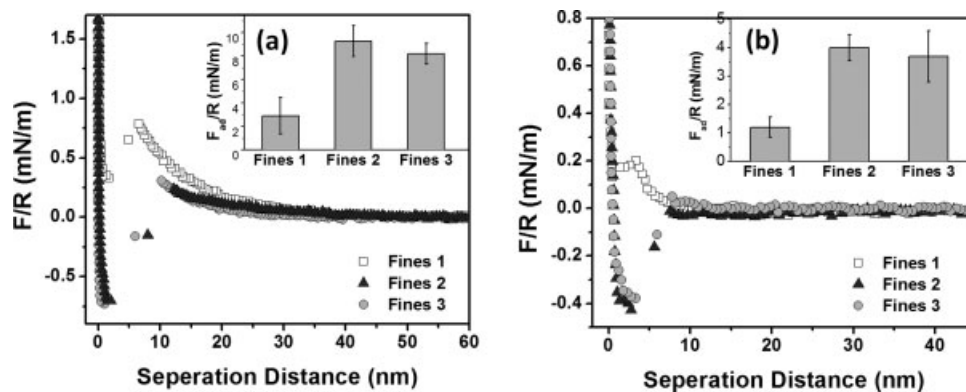


**Figure 5. Normalized long-range interaction forces ( $F/R$ ) between bitumen and various fine solids: Good ore fines (Fines 1), laboratory weathered ore fines (Fines 2), and naturally weathered ore fines (Fines 3) as a function of separation distance in (a) 1 mM KCl solutions and (b) plant process water at pH = 8.0–8.6.**

Inset shows the corresponding normalized adhesion forces.

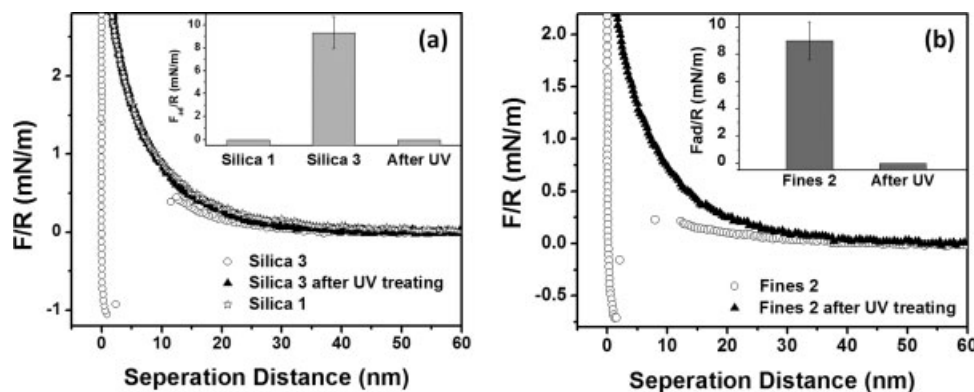


**Figure 6.** Normalized long-range interaction forces ( $F/R$ ) as a function of separation distance for bitumen interacting with (a) the weathered silica (Silica 3), and (b) fines from laboratory weathered ores (Fines 2) before and after UV treatment. 1 mM KCl solutions of pH = 8.0–8.6 were used as the test liquid medium. Inset shows the corresponding normalized adhesion forces.

adhesion forces by hot water washing are anticipated to improve the processability of the weathered ores.

## Discussion

The classical DLVO theory has been successfully used to describe the colloidal interactions between two colloidal surfaces. In the classical DLVO theory, only electrostatic double layer force ( $F_E$ ) and van der Waals forces ( $F_V$ ) are considered:<sup>12,21,22</sup>

$$F_{DLVO} = F_E + F_V \quad (1)$$

Given a sphere of radius  $R$  interacting with a flat surface, the van der Waals forces can be calculated using the following equation:

$$\frac{F_V}{R} = -\frac{A}{6D^2} \quad (2)$$

where  $A$  is the Hamaker constant and  $D$  is the separation distance between the two interacting surfaces. The electrostatic double-layer forces, on the other hand, were calculated by numerically solving nonlinear Poisson-Boltzmann (PB) Eq. 3, at constant surface potential boundary conditions. The PB equation was solved in the form of interaction force per unit area ( $F(x)$ ) given in Eq. 4, which is integrated to get energy per area between two planar plates ( $U_E(D)$ ) given by Eq. 5. Finally, Derjaguin's approximation of Eq. 6 was used to calculate the electrical double-layer forces ( $F_E(D)$ ) between a sphere and a flat plate at separation distance  $D$ .

$$\varepsilon \varepsilon_0 \frac{d^2 \psi}{dx^2} = -e \sum_i z_i n_{i\infty} \exp\left(\frac{-z_i e \psi}{k_B T}\right) \quad (3)$$

$$F(x) = k_B T \sum_i n_{i\infty} \left( \exp\left(\frac{-z_i e \psi}{k_B T}\right) - 1 \right) - \frac{\varepsilon \varepsilon_0}{2} \left( \frac{d\psi}{dx} \right)^2 \quad (4)$$

$$U_E = - \int_{\infty}^D F(h) dh \quad (5)$$

$$\frac{F_E(D)}{R} = 2\pi U_E(D) \quad (6)$$

In Eqs. 3 and 4,  $\varepsilon$  and  $\varepsilon_0$  are permittivity of medium and vacuum, respectively;  $e$  is the elementary electric charge;  $z$  is the valence of  $i^{\text{th}}$  electrolyte;  $n_{i\infty}$  is the bulk concentration of  $i^{\text{th}}$  electrolyte;  $k_B$  is the Boltzmann constant;  $\psi$  is the surface electric potential;  $h$  is separation distance; and  $T$  is temperature. A Visual Basic program running on an Excel spreadsheet was developed to theoretically calculate the DLVO forces.<sup>11</sup>

In addition to the electrostatic double layer force ( $F_E$ ) and van der Waals forces ( $F_V$ ), an attractive force referred to as long-range hydrophobic force has been reported to exist between two hydrophobic surfaces in an aqueous medium,<sup>23–28</sup> which could be described by an empirical equation given below,<sup>12</sup>

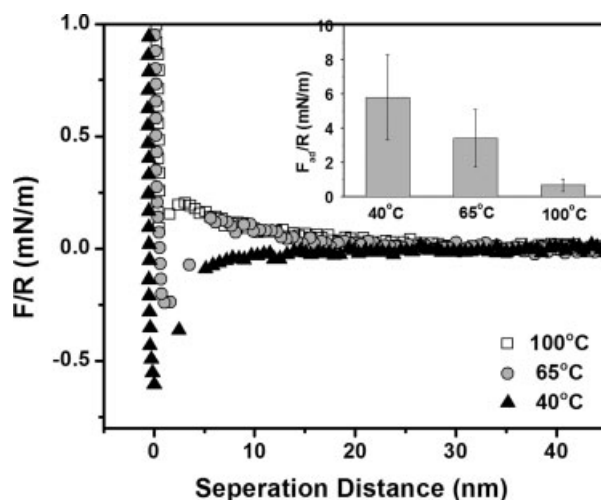


**Figure 7.** Effect of hot water washing of the laboratory weathered ore fines (Fines 3) on its interaction with bitumen in 1 mM KCl solutions at pH = 8.0–8.6. Inset shows the corresponding adhesion forces.

**Table 4. Measured Zeta Potentials of Plant Extracted Bitumen Droplets and Silica Particles in 1 mM KCl Solutions and Industrial Plant Process Water at pH 8.0–8.6**

Samples		Plant Bitumen	Silica 1
Zeta Potential (mV)	In 1 mM KCl	$-72 \pm 9$	$-56 \pm 4$
	In PW	$-35 \pm 3$	$-20 \pm 2$

$$\frac{F_H}{R} = -\frac{K}{6D^2} \quad (7)$$

where  $K$  is an empirical parameter whose value depends on the hydrophobicity of interacting surfaces. Including the hydrophobic forces in the classical DLVO theory leads to a so-called extended DLVO (E-DLVO) theory given by Eq. 8

$$F_{E-DLVO} = F_E + F_V + F_H \quad (8)$$

Because of the shape irregularity of the fine solids as shown in Figure 1, the theoretical analysis was performed only on bitumen interacting with silica particles of well-defined shape. In the calculations of DLVO or E-DLVO forces, the decay length values of 9.6 and 1.8 nm, were obtained using Debye-Hückel theory<sup>21</sup> for 1 mM KCl solution and the plant process water, respectively, while the Hamaker constant of  $3.3 \times 10^{-21}$  J for the silica(fines)/water/bitumen system was used.<sup>11,15</sup> For bitumen interaction with hydrophilic Silica 1, Eq. 1 was used to calculate the interaction forces. The measured zeta potential values of bitumen and hydrophilic silica powder (Silica 1), given in Table 4, were used as approximation of their corresponding Stern potentials ( $\psi$ ) to calculate the electric double layer forces. The calculated DLVO force profiles agreed well with the measured force profiles as shown in Figure 2, indicating the absence of hydrophobic forces in the current system. This is an important finding as it allows us to determine the Stern potential of Silica 2 and Silica 3 using a hydrophilic model silica probe in AFM colloidal force measurements as describe below.

Because the number of silica particles (Silica 2 and Silica 3) mixed and then extracted from oil sands were very limited, direct measurement of their zeta potentials was not performed. Instead, colloidal probe technique was used to determine Stern potentials of Silica 2 and Silica 3. Because we established the absence of non-DLVO forces when a hydrophilic silica probe interacts with a hydrophobic bitumen, the interaction forces between a model hydrophilic silica probe and Silica 1, Silica 2, or Silica 3 in a simple electrolyte solution and process water were measured. The results are given in Figure 8. The measured force profiles are fitted with the classical DLVO theory. In 1 mM KCl solutions of pH 8.0–8.6, the zeta potential of the hydrophilic silica probe is known ( $-56$  mV as measured using the electrophoresis method). By best fitting the measured force profile in Figure 8a to the classical DLVO theory, the only unknown parameter, the Stern potential of the substrate, is determined to be  $-54$  mV for Silica 1,  $-47$  mV for Silica 2, and  $-40$  mV for Silica 3. The results summarized in Table 5 show that the fitted Stern potential of Silica 1 is very close to the measured zeta potential values of hydrophilic silica powders ( $-56$  mV in Table 4), as anticipated. In contrast, the fitted Stern potentials for Silica 2 and Silica 3 are different from the values of the untreated silica, indicating not only the adsorption of organic materials from bitumen on silica particles and subsequent weathering of adsorbed organic materials, but also the impact of the adsorbed organic materials on zeta potential of silica. In the process water, little deviation among the measured force profiles was observed (Figure 8b). Through the best fit of the measured force profiles to the classical DLVO theory, the zeta potentials of the three types of silica surfaces were determined to be about  $-20$  mV. This value is identical to the measured zeta potential of silica powders in the same plant process water using the electrophoresis method (Table 4). More importantly, the measured colloidal force profiles can be well fitted by the classical DLVO theory for all the cases in Figure 8, confirming the absence of hydrophobic force and hence the suitability of obtaining Stern potential values by fitting the measured force profiles between a hydrophilic model probe of known Stern (or zeta-) potential and other surfaces. The

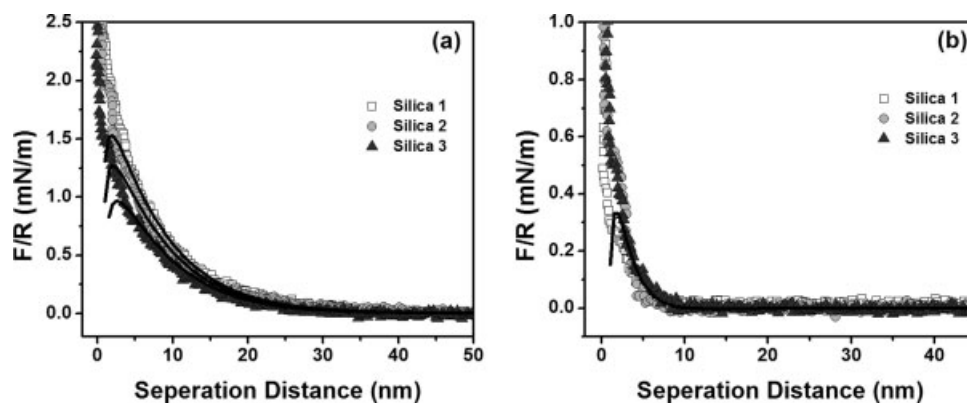


**Figure 8. Normalized long-range interaction forces ( $F/R$ ) of model hydrophilic silica probe interacting with hydrophilic model silica (Silica 1), nonweathered model silica (Silica 2) and weathered model silica (Silica 3) as a function of separation distance in (a) 1 mM KCl solutions and (b) plant process water at pH = 8.0–8.6.**

Solid lines represent the best fitted classical DLVO force profiles.

Stern potential values obtained in this manner are used in the calculation of electrical double layer forces between bitumen and Silica 2 or Silica 3 in electrolyte solutions or process water.

When the Stern potential values of silica particles as determined above were used to fit the measured force profiles between bitumen and Silica 2 or Silica 3, it was found that the classical DLVO theory overestimated the interaction forces, indicating the existence of extra attractive forces in such systems. In our previous wettability study, the solids from weathered ores were found to be hydrophobic.<sup>17</sup> As the bitumen surface was also hydrophobic, an attractive hydrophobic force was anticipated to exist between the hydrophobic Silica 2 or Silica 3 and bitumen. After introducing the extra hydrophobic forces, the force profiles in Figure 3 for bitumen interacting with bitumen-coated model silica spheres without (Silica 2) or with (Silica 3) laboratory weathering can be well fitted with the extended DLVO theory. The  $K$  values obtained by best fitting are summarized in Table 6. In 1mM KCl solutions, the  $K$  values are  $20 \times 10^{-21}$  and  $100 \times 10^{-21}$  J for Silica 2 and Silica 3, respectively. These values are much greater than the Hamaker constant value of  $3.3 \times 10^{-21}$  J, suggesting that the attractive hydrophobic forces are much stronger than van der Waals forces between hydrophobic surfaces in aqueous solutions. Clearly, the observed weak repulsive force or strong attractive force between bitumen and Silica 2 or Silica 3 is closely linked with the increased hydrophobicity of silica by the contact with bitumen and subsequent weathering, as determined by increased contact angle values on the silicon surfaces in the previous study.<sup>17</sup> The hydrophobic force between bitumen and a hydrophobized model silica by silanation was reported by Liu et al.<sup>6</sup> In the plant process water, the corresponding  $K$  values were decreased to  $15 \times 10^{-21}$  and  $40 \times 10^{-21}$  J for Silica 2 and Silica 3, respectively (Table 6). The reasons for the decrease in the attractive hydrophobic force in the process water were not clear due to the complexity of the industrial process water. The presence of surfactant in the process water likely contributes to such decrease in hydrophobic forces.

With increasing surface hydrophobicity of the solids, unfavourable attractive forces between the hydrophobic surfaces would lead to an increase in adhesion between bitumen and solids.<sup>24</sup> Therefore, the observed increase in adhesion between bitumen and silica after being mixed with the oil sands ore and subsequent weathering is not unexpected. The reduction in the magnitude of the attractive hydrophobic force in process water compared with that in simple electrolyte solutions of lower ionic strength would also lead to a reduced adhesion as observed in this study. Hot water washing was observed to significantly reduce hydrophobicity of weathered solids.<sup>17</sup> As a result, the adhesion force between bitumen and the washed

**Table 5. Stern Potential (mV) of Silica Surfaces in 1 mM KCl Solutions and Industrial Plant Process Water at pH = 8.0–8.6, Derived from the Best Fit of the Measured Force Profiles of These Silica Surfaces Interacting with a Hydrophilic Probe**

Solution	Silica 1	Silica 2	Silica 3
1 mM KCl	$-54 \pm 3$	$-47 \pm 2$	$-40 \pm 2$
PW	$-20 \pm 2$	$-20 \pm 2$	$-20 \pm 2$

**Table 6. The Hydrophobic Force Constant,  $K$  ( $\times 10^{-21}$  J), Used to Fit the Long-Range Forces between Bitumen and Various Model Silica Spheres in 1 mM KCl Solutions and Plant Process Water**

Solution	Silica 1	Silica 2	Silica 3
1 mM KCl	0	$20 \pm 8$	$100 \pm 15$
PW	0	$15 \pm 5$	$40 \pm 10$

solids decreased significantly. It is clear that the poor processability of weathered ores is a consequence of observed increase in solids hydrophobicity which leads to lower bitumen liberation and possible slime coating. Because hot water washing leads to a decrease in the attractive hydrophobic and adhesion forces between bitumen and solids, high processing temperature is anticipated to improve oil sands processability. Indeed, it is well documented in literature and established in practice that higher processing temperature provides a higher bitumen recovery.<sup>29–31</sup>

## Conclusions

The study by AFM colloidal force measurements showed that oil sands weathering has a profound effect on the interaction forces between bitumen and solids in 1 mM KCl solutions and process water, changing the long-range interaction from strongly repulsive to attractive and significantly increasing the adhesion force. The results of the measurements using well-defined model silica spheres after being mixed with an oil sands ore and their subsequent laboratory weathering proved such an effect. Theoretical analysis with model silica revealed the presence of additional attractive forces, which are attributed to the hydrophobic force arising from the hydrophobization of the solids during weathering. Strong attractive long-range and adhesion forces between bitumen and solids from weathered ores would lead to poor bitumen liberation from the sand grains, thereby accounting for poor processability of weathered ores. Hot-water washing of the solids counteracts the weathering effects, and partially restores the repulsive long-range forces and decreases adhesion forces, thereby providing an avenue for improving the processability of weathered ores using a higher processing temperature.

## Acknowledgments

The authors acknowledge the financial support from the NSERC Industrial Research Chair in Oil Sands Engineering (held by J. H. Masliyah.).

## Literature Cited

- Bowman CW. *Molecular and Interfacial Properties of Athabasca Tar Sands*. Presented at: 7th World Petroleum Congress Processing, 1967:583–604.
- Mikula RJ, Munoz VA, Wang N. Characterization of bitumen properties using microscopy and near infrared spectroscopy: processability of oxidized or degraded ores. *J Can Pet Technol*. 2003;42:50–54.
- Sanford EC. Processability of athabasca oil sand: interrelationship between oil sand fine solids, process aids, mechanical energy and oil sand age after mining. *Can J Chem Eng*. 1983;61:554–567.
- Wallace D, Henry D. *Aging of Oil Sand During Storage, Engineering Foundation Conference on the Processing of Energy Minerals: Shale, Tar Sands and Coal*. New Hampshire: Henniker, 1984.



5. Wallace D, Henry D, Takamura K. A Physical chemical explanation for deterioration in the hot water processability of athabasca oil sand due to aging. *Fuel Sci Tech Int.* 1989;7:699–725.
6. Liu JJ, Xu ZH, Masliyah J. Processability of oil sand ores in Alberta. *Energy Fuels.* 2005;19:2056–2063.
7. Clark KA. Hot-water separation of Alberta bituminous sand. *Trans Can Inst Min Metall.* 1944;47:257–274.
8. Masliyah J, Zhou ZJ, Xu ZH, Czarnecki J, Hamza H. Understanding water-based bitumen extraction from athabasca oil sands. *Can J Chem Eng.* 2004;82:628–654.
9. Liu JJ, Xu ZH, Masliyah J. Interaction forces in bitumen extraction from oil sands. *J Colloid Interface Sci.* 2005;287:507–520.
10. Li HH, Long J, Xu ZH, Masliyah JH. Synergetic role of polymer flocculant in low-temperature bitumen extraction and tailings treatment. *Energy Fuels.* 2005;19:936–943.
11. Liu JJ, Xu ZH, Masliyah J. Studies on bitumen-silica interaction in aqueous solutions by atomic force microscopy. *Langmuir.* 2003;19:3911–3920.
12. Ploehn HJ, Liu C. Quantitative analysis of montmorillonite platelet size by atomic force microscopy. *Ind Eng Chem Res.* 2006;45:7025–7035.
13. Long J, Xu ZH, Masliyah JH. On the role of temperature in oil sands processing. *Energy Fuels.* 2005;19:1440–1446.
14. Long J, Zhang LY, Xu ZH, Masliyah JH. Colloidal interactions between langmuir-blodgett bitumen films and fine solid particles. *Langmuir.* 2006;22:8831–8839.
15. Zhao HY, Long J, Masliyah JH, Xu Z. H.. Effect of divalent cations and surfactants on silica-bitumen interactions. *Ind Eng Chem Res.* 2006;45:7482–7490.
16. Liu JJ, Xu ZH, Masliyah J. Interaction between bitumen and fines in oil sands extraction system: implication to bitumen recovery. *Can J Chem Eng.* 2004;82:655–666.
17. Ren SL, Trong DV, Zhao HY, Long J, Xu ZH, Masliyah J. Effect of weathering on surface characteristics of solids and bitumen from oil sands. *Energy Fuels.* 2009;23:2628–2636.
18. Clear SC, Nealey PF. Lateral force microscopy study of the frictional behavior of self-assembled monolayers of octadecyltrichlorosilane on silicon/silicon dioxide immersed in n-alcohols. *Langmuir.* 2001;17:720–732.
19. Ren SL, Yang SR, Zhao YP, Yu TX, Xiao XD. Preparation and characterization of an ultrahydrophobic surface based on a stearic acid self-assembled monolayer over polyethyleneimine thin films. *Surf Sci.* 2003;546:64–74.
20. Liu JJ, Zhou Z, Xu ZH. Electrokinetic study of hexane droplets in surfactant solutions and process water of bitumen extraction systems. *Ind Eng Chem Res.* 2002;41:52–57.
21. Israelachvili JN. *Intermolecular and Surface Forces*, 2nd ed. London, England: Academic Press, 1992.
22. Masliyah JH. *Electrokinetic Transport Phenomena*. AOSTRA Technical Publication Series No. 12. Edmonton, Alberta: Alberta Oil Sands Technology and Research Authority, 1994.
23. Meyer EE, Rosenberg KJ, Israelachvili J. Recent progress in understanding hydrophobic interactions. *Proc Natl Acad Sci USA.* 2006;103:15739–15746.
24. Skvarla J. Hydrophobic interaction between macroscopic and microscopic surfaces. Unification using surface thermodynamics. *Adv Colloid Interface Sci.* 2001;91:335–390.
25. Ducker WA, Senden TJ, Pashley RM. Direct measurement of colloidal forces using an atomic force microscope. *Nature.* 1991;353:239–241.
26. Nguyen AV, Nalaskowski J, Miller JD, Butt HJ. Attraction between hydrophobic surfaces studied by atomic force microscopy. *Inter J Miner Process.* 2003;72:215–225.
27. Teschke O, de Souza EF. Measurements of long-range attractive forces between hydrophobic surfaces and atomic force microscopy tips. *Chem Phys Lett.* 2003;375:540–546.
28. Kotlyar LS, Sparks BD, Woods J, Capes CE, Schutte R. Biwetted ultrafine solids and structure formation in oil sands fine tailings. *Fuel.* 1995;74:1146–1149.
29. Dai Q, Chung KH. Bitumen-sand interaction in oil sand processing. *Fuel.* 1995;74:1858–1864.
30. Hepler LG, Hsi C. *AOSTRA Technical Handbook on Oil Sands, Bitumens and Heavy Oils*. Edmonton, AB: Alberta Oil Sands Technology and Research Authority, 1989.
31. Isaacs EE, Morrison DN. Interfacial films at the athabasca bitumen/water interface. *AOSTRA J Res.* 1985;2:113–119.

Manuscript received Dec. 18, 2008, and revision received Jun. 1, 2009.